Imaging a functional tumorigenic biomarker in the transformed epithelium

Aaron M. LeBeau[a,b], Minhee Lee[c], Stephanie T. Murphy[b], Byron C. Hann[d], Robert S. Warren[d], Romelyn Delos Santos[b], John Kurhanewicz[b], Samir M. Hanash[c], Henry F. VanBrocklin[b,1], and Charles S. Craik[a,1]

[a]Department of Pharmaceutical Chemistry, University of California, San Francisco, CA 94158; [b]Center for Molecular and Functional Imaging, Department of Radiology and Biomedical Imaging, University of California, San Francisco, CA 94107; [c]Division of Public Health Sciences, Fred Hutchinson Cancer Research Center, Seattle, WA 98109; and [d]Helen Diller Family Comprehensive Cancer Center, University of California, San Francisco, CA 94115

Edited by Michael A. Marletta, University of California, Berkeley, CA, and approved November 16, 2012 (received for review October 30, 2012)

Proteases responsible for the increased peritumoral proteolysis associated with cancer represent functional biomarkers for monitoring tumorigenesis. One attractive extracellular biomarker is the transmembrane serine protease matriptase. Found on the surface of epithelial cells, the activity of matriptase is regulated by its cognate inhibitor hepatocyte growth factor activator inhibitor-1 (HAI-1). Quantitative mass spectrometry allowed us to show that, in selected cancers, HAI-1 expression decreases, leading to active matriptase. A preclinical probe specific for the measurement of emergent active matriptase was developed. Using an active-site–specific, recombinant human antibody for matriptase, we found that the selective targeting of active matriptase can be used to visualize the tumorigenic epithelium. Live-cell fluorescence imaging validated the selectivity of the antibody in vitro by showing that the probe localized only to cancer cell lines with active matriptase on the surface. Immunofluorescence with the antibody documented significant levels of active matriptase in 68% of primary and metastatic colon cancer sections from tissue microarrays. Labeling of the active form of matriptase in vivo was measured in human colon cancer xenografts and in a patient-derived xenograft model using near-infrared and single-photon emission computed tomography imaging. Tumor uptake of the radiolabeled antibody, ^{111}In-A11, by active matriptase was high in xenografts (28% injected dose per gram) and was blocked in vivo by the addition of a matriptase-specific variant of ecotin. These findings suggest, through a HAI-1–dependent mechanism, that emergent active matriptase is a functional biomarker of the transformed epithelium and that its proteolytic activity can be exploited to noninvasively evaluate tumorigenesis in vivo.

cancer biomarker | molecular imaging

Proteolysis is a posttranslation modification (PTM) that, unlike other PTMs such as phosphorylation, methylation, and ubiquitination, cannot be reversed. This irreversible process can become dysregulated during the progression of human cancers. Protease networks are known to promote the growth and survival of cancer cells by activating promitotic cytokines and growth factors, resulting in cancer with an aggressive phenotype (1). It has also been well documented that a host of proteases degrade components of the extracellular matrix, leading ultimately to cancer metastasis (2–4). A hallmark of cancer is increased pericellular proteolytic activity in tumor tissue and the surrounding microenvironment resulting from protease overexpression, mislocalization, and/or a decrease in the expression levels of macromolecular protease inhibitors. The proteases responsible for the increased proteolytic activity represent candidate biomarkers that can be leveraged for diagnostic/prognostic purposes using active-site specific probes. The levels of such biomarkers could be used as a metric for judging the therapeutic efficacy of treatments and for stratifying patients into different treatment cohorts, leading to more effective personalized therapeutic regimens.

One candidate protease biomarker ubiquitously expressed in adenocarcinomas is matriptase (5–7). Matriptase, also referred to as MT-SP1, ST14, TADG-15, and PRSS14, is a trypsin-like protease and a member of the type II transmembrane serine protease (TTSP) family. The role that matriptase, which is expressed on the surface of cancerous epithelial cells, plays in cancer is unclear; however, matriptase has been shown to cleave a number of cancer-promoting substrates from growth factors to basement membrane proteins (8, 9). In addition to adenocarcinomas, studies have implicated matriptase in the initiation of oncogenic activity in squamous cell carcinoma models (10). Matriptase is expressed in a range of normal human tissue types with high transcript levels found in the colon, rectum, and pancreas (11). In healthy tissue, matriptase is responsible for regulating barrier formation in the skin, intestines, and during embryonic development (10, 12, 13). The proteolytic activity of matriptase is closely regulated by its cognate macromolecular inhibitor hepatocyte growth factor activator inhibitor-1 (HAI-1) (8). Matriptase and HAI-1 are coexpressed and colocalized on the extracellular surface. In normal tissue, the ratio of matriptase to HAI-1 is low, resulting in little matriptase-mediated proteolysis (14). The matriptase/HAI-1 ratio increases during the progression of certain cancers, resulting in a population of active matriptase on the cell surface (15).

Proteolytic activity has been confirmed as a viable marker for cancer imaging in vivo using near-infrared (NIR) and nuclear imaging modalities (16–18). Most approaches have used small-molecule probes that target either metallo- or cysteine proteases. Targeting proteases with small molecules for imaging is challenging due to the physical properties of different radionuclides, chelate groups, and fluorophores. Slight structural modifications of small molecules can drastically affect pharmacokinetics, leading to probes of limited utility (19). Also, there is a paucity of electrophilic warheads available for targeting serine proteases in complex environments that have favorable reaction kinetics and low toxicity (20, 21). Antibodies provide an alternative to small molecules for targeting serine proteases in vivo. Antibodies can be functionalized for multiple imaging modalities with limited change in their pharmacokinetics. The multiple points of contact made by antibodies with target proteases allows for the engineering of antibodies that can selectively and potently inhibit individual members of large protease families (22). There are a growing number of antibody-based platforms for cancer detection and treatment that have been Federal Drug Administration-approved such as ProstaScint, Bexxar, Zevalin, and Herceptin (18, 23, 24).

Previously, our laboratory reported the development of an active-site specific macromolecular probe for matriptase. Using

Author contributions: A.M.L., M.L., H.F.V., and C.S.C. designed research; A.M.L., M.L., S.T.M., and R.D.S. performed research; A.M.L., M.L., S.T.M., B.C.H., R.S.W., R.D.S., J.K., S.M.H., H.F.V., and C.S.C. contributed new reagents/analytic tools; A.M.L., M.L., S.T.M., H.F.V., and C.S.C. analyzed data; and A.M.L., M.L., H.F.V., and C.S.C. wrote the paper.

The authors declare no conflict of interest.

This article is a PNAS Direct Submission.

[1]To whom correspondence may be addressed. E-mail: charles.craik@ucsf.edu or henry.vanbrocklin@ucsf.edu.

This article contains supporting information online at www.pnas.org/lookup/suppl/doi:10.1073/pnas.1218694110/-/DCSupplemental.

a human fragment of antigen binding (Fab) phage display library, a human monoclonal antibody that could selectively recognize the active form of matriptase was discovered (25, 26). The lead antibody, A11, was converted from the Fab to the larger and more potent IgG with a K_i of 35 pM and showed no cross-reactivity with matriptase zymogen, HAI-1–bound matriptase, or the murine matriptase ortholog epithin (27). In this report, the use of an antibody probe to detect active matriptase and elucidate a mechanism for its activity in human cancer models is described. Our probe was able to image active matriptase in cancer cell lines in vitro and in experimental xenografts in vivo. Immunofluorescence using colon cancer tissue microarrays documented high levels of active matriptase in every stage of disease, but not in healthy tissue. These results indicate that active matriptase is a cancer-specific marker and that the single-photon emission computed tomography (SPECT) imaging of functional biomarkers, with antagonistic antibodies, could be a viable strategy for detecting cancer in the clinic.

Results

Detection and Quantification of Active Matriptase in Vitro. The mechanism and rationale behind the ability of the human antibody A11 to detect the active form of matriptase in cancer was investigated. Cell lines derived from adenocarcinomas known histologically to express matriptase were surveyed with AlexaFluor 488-labeled A11 IgG (A11-AF488) using live-cell fluorescence microscopy. The eight cancer cell lines analyzed included four colon (HT29, SW480, SW620, and HCT116), two pancreatic (AsPC-1 and CFPAC-1), and two breast cancer (SKBR3 and MDA-MB-231) cell lines. Of the eight cell lines investigated, three cell lines—HT29, SW480, and CFPAC-1—demonstrated significant A11-AF488 localization to the cell membrane where active matriptase is located (Fig. 1). Quantitative in-depth proteomic profiling by liquid chromatography–mass spectrometry (LC-MS)/MS was applied to the eight cancer cells lines to measure the levels of matriptase and HAI-1 on the cell surface using a MS2 spectral counting method (Fig. 2*A*) (28–30). Using this approach, the three cell lines that demonstrated probe localization were found to have the highest matriptase protein expression with HT29 possessing the most. The MS2 spectral counts for HAI-1 protein were lower than matriptase in the three cell lines, resulting in matriptase/HAI-1 protein ratios of 1.21 for HT29, 1.25 for CFPAC-1, and 1.19 for SW480. The cell lines HT29, CFPAC-1, and SW480 had the following active matriptase spectral counts (AMSC): AMSC = MS2 spectral counts of matiptase$_{total}$ − MS2 spectral counts of HAI-1$_{total}$) of 50, 37, and 12, respectively. The other cell lines had greater HAI-1 protein expressed on the cell surface with matriptase/HAI-1 protein ratios ranging from 0.5 to 0.08. MDA-MB-231 was the only cell line with no detectable matriptase.

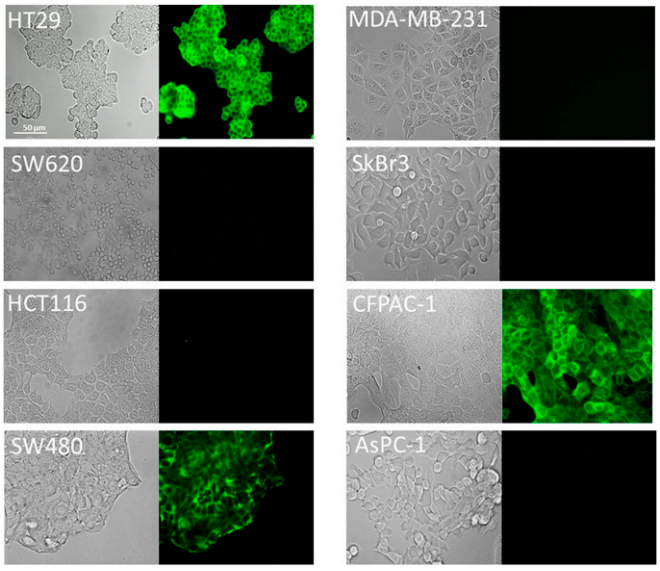

Fig. 1. Live-cell fluorescence imaging with A11-AF488. Four colon cancer cell lines (HT29, SW620, HCT116, and SW480), two breast (MDA-MB-231 and SkBr3), and two pancreatic (CFPAC-1 and AsPC-1) cell lines were grown in cell culture and treated with 100 nM of A11-AF488. After 2 h, the cells were washed and imaged. (*Left*) Bright-field image of the cells. (*Right*) FITC channel. Localization of A11-AF488 in the FITC channel (green) was observed in HT29, SW480, and CFPAC-1.

Analysis of the eight cell lines using quantitative PCR (qPCR) revealed findings concordant with the mass spectrometry data (Fig. 2*B*). qPCR analysis documented that HT29, CFPAC-1, and SW480 had the highest levels of matriptase mRNA present and were the only three with matriptase expression greater than HAI-1 expression. Because two of the three cancer cell lines that demonstrated probe localization were of colon origin, mRNA expression was analyzed in colon tissue to see if the matriptase/HAI-1 mRNA ratio was of clinical significance (Fig. 2*C*). The mRNA ratio of matriptase to HAI-1 was found to increase from normal colon to premalignant adenoma tissue ($P = 0.03$). A significant increase in the ratio was observed between normal colon and stage II tumor tissue ($P < 0.0001$) and metastatic tumor tissue from hepatic lesions ($P = 0.0002$). The level of HAI-1 mRNA had decreased 75% in the stage II tissue compared with normal colon.

The significance of active matriptase at the protein level in colon cancer was further documented using immunofluorescence. Immunofluorescence was performed on formalin-fixed paraffin-embedded (FFPE) healthy human colon sections with A11-AF488 and a polyclonal matriptase/ST14 antibody (Bethyl) that recognizes a C-terminal epitope of matriptase. The matriptase/ST14 antibody identifies the total amount of matriptase present in the tissue—matriptase in zymogen form, active matriptase, inactive structural variants, and matriptase complexed to HAI-1. In Fig. 3*A*, the matriptase/ST14 antibody found matriptase present on the surface of goblet cells seen in the FITC channel. E-cadherin was stained and visualized in the Cy3 channel to delineate the epithelium. The matriptase/ST14 antibody did not show any reactivity with stromal components, reaffirming data documenting that matriptase is an epithelium specific marker (12). The active-site specific A11-AF488 did not detect active matriptase in the healthy colon tissue (Fig. 3*B*). Active matriptase was detected in primary colon cancer tissues from tissue microarrays using A11-AF488 (Fig. S1). Depicted in Fig. 3*C* is a moderately differentiated stage II (T3N1M0) section stained with A11-AF488 showing active matriptase expressed in the epithelium. From the microarray data, active matriptase was found in adenocarcinomas of every stage (stages I–IV) and in tissues that were well to moderately differentiated (Fig. S1). Of 152 unique primary and metastatic tissue cores examined, 104 cores (68%) were found to have active matriptase. Active matriptase was not detected in any human lymph node metastases surveyed ($n = 10$). Sections of hepatic metastases, used to establish the patient-derived xenograft (PDX) model for SPECT imaging, were stained for active matriptase with A11-AF488 (Fig. 3*D*). Active matriptase was found coexpressed along with E-cadherin in the hepatic metastasis tissue. Normal hepatic tissue expressed low levels of E-cadherin and no active matriptase (Fig. S1).

Imaging Active Matriptase in Preclinical Animal Models. Imaging active matriptase was performed in colon cancer xenografts possessing levels of high, low, and no active matriptase. The presence of active matriptase was first qualitatively assessed in vivo using NIR optical imaging. A11 IgG labeled with the NIR fluorophore AlexaFluor 680 (A11-AF680) was administered to mice bearing HT29 (50 AMSC), SW480 (12 AMSC), and SW620 (0 AMSC)

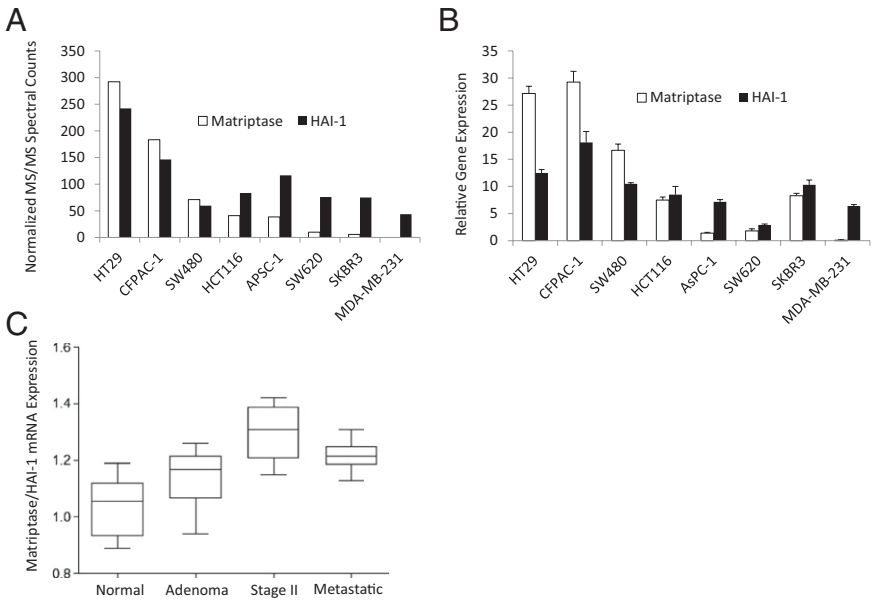

Fig. 2. Quantification and analysis of matriptase/HAI-1 protein and gene expression. (*A*) Cell lines for live-cell imaging were subjected to quantitative proteomic profiling analysis after stable isotope labeling with amino acids in cell culture to determine the relative quantities of matriptase and HAI-1 on the cell surface. More spectral counts for matriptase than for HAI-1 were detected in HT29, SW480, and CPFAC-1. (*B*) mRNA analysis of matriptase and HAI-1 in the cancer cell lines as measured by qPCR. (*C*) Boxplot depicting normalized matriptase/HAI-1 mRNA expression in healthy, premalignant, and malignant colon tissue shows an increase in matriptase/HAI-1 mRNA as cancer progresses. Each box represents $n = 16$ clinical tissue samples.

xenografts ($n = 3$ mice/xenograft) and imaged serially every 24 h to assess tumor localization and biodistribution (Fig. 4*A*). Maximum probe uptake and retention was observed in the HT29 xenograft at 72 h. Significantly less tumor uptake was observed in SW480, in accordance with the measured protein levels, whereas SW620 demonstrated no probe localization in vivo. At 72 h, selected HT29, SW480, and SW620 mice were euthanized, and the tumors were resected and imaged to evaluate probe penetration in the tumor. The resected HT29 tumors showed the greatest probe penetration and fluorescence.

The preclinical utility of A11 IgG for the detection and quantitation of active matriptase in vivo was investigated using the nuclear imaging modality SPECT. For SPECT imaging, A11 was labeled on lysine residues with a bifunctional 1,4,7,10-tetraazacyclododecane-1,4,7,10-tetraacetic acid (DOTA) chelate derivative (A11-DOTA) and then with the gamma-emitting radionuclide ^{111}In ($t_{1/2} = 2.8$ d). The $^{111}InCl_3$ labeling yield of A11-DOTA, used to create ^{111}In-A11, was found to be 87%. Labeling A11-DOTA with ^{111}In had no effect on the K_i of the antibody for matriptase. The radiochemical purity of the final injected product was greater than 97%. Mice ($n = 3$/xenograft) were imaged with a small animal SPECT/X-ray computed tomography (SPECT/CT) starting 24 h post injection. According to the time-activity curve for the HT29 xenograft, tumor uptake was at its zenith 72 h post injection (Fig. 4*B* and Fig. S2). Ecotin, a macromolecular protease inhibitor originally isolated from bacteria in the human gut, inhibits several serine proteases. Ecotin-RR, engineered as a selective competitive inhibitor of matriptase with a K_i value in the low picomolar range, was administered to mice bearing an HT29 xenograft to prevent ^{111}In-A11 localization in vivo. Ecotin-RR blocked uptake of the probe as evidenced by a diminished scintigraphic signal from the tumor location and increased hepatic clearance (Fig. 4*B*). Probe accumulation was observed in the SW480 xenograft to a lesser extent than HT29 (Fig. 4*B*). No probe uptake was observed in the control SW620 mice (Fig. S3).

The intrinsic tumor heterogeneity of colon cancer cannot be replicated using clonally derived cell-line xenografts that are genotypically and phenotypically homogenous; therefore, ^{111}In-A11 was tested in a PDX model. The PDX model was created using resected tumor tissue from the hepatic metastases of a colon cancer patient (*SI Methods*). The tumor tissue was implanted, grown, and serially passaged in mice. The ability of PDX models to reproduce the diversity observed in human tumors has been validated (31). At 72 h, ^{111}In-A11 showed pronounced uptake in PDX tumors derived from the same patient lineage (Fig. 4*B*). Following probe washout, the PDX mice ($n = 3$) were euthanized and their tumors were harvested. Immunofluorescence using A11-AF488 was performed on tumor sections to detect active matriptase (Fig. S4). Active matriptase was detected in all of the sections from the three mice imaged with SPECT. Although the limited availability of this model precluded a large biodistribution study of ^{111}In-A11, immunofluorescence with A11-AF488 was performed on archived PDX sections derived from different patient lineages and passage numbers (Fig. S5). Active matriptase was detected in 12/12 (100%) sections that originated from 10 patients, indicating the broad potential of this probe. Importantly, A11-AF488 was able to detect active matriptase in both frozen tissue and FFPE sections.

A biodistribution study with ^{111}In-A11 was performed at 24, 48, and 72 h in HT29 xenograft mice (Fig. 5*A*). At 72 h, tumor uptake was 28.3% injected dose per gram (ID/g), greater than for all other organs and tissues studied. The 72-h tumor/muscle ratio was 93, and the tumor/blood ratio was 9. IgG antibodies clear through the hepatic system and tend to accumulate in the spleen; this was seen in the study, but the uptake in both organs was 50% less than the accumulation observed in the tumor (18). The blocking study with Ecotin-RR resulted in a greater than 80% decrease in ^{111}In-A11 uptake in the tumor. No appreciable accumulation was observed in the intestines where the murine ortholog epithin is known to be present, further corroborating the specificity of A11 for human matriptase. Tumor uptake was also measured at 72 h in the low-active matriptase xenograft, SW480, and two negative controls (SW620 and MDA-MB-231) (Fig. 5*B*). SW620 had a tumor uptake of 12.4% whereas SW620 and MDA-MB-231 have values of 3.19% and 2.2% representing nonspecific tumor uptake and retention. From these results it was possible to directly correlate tumor

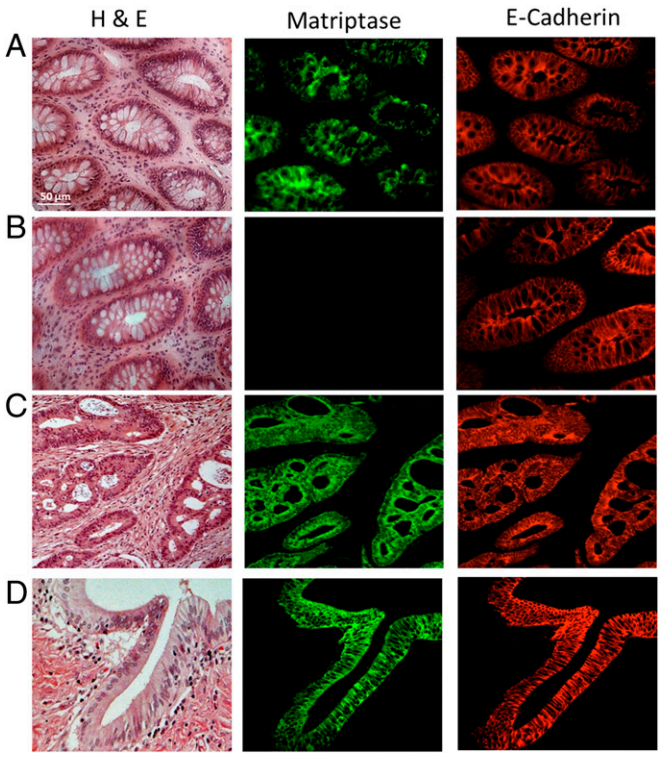

Fig. 3. Visualizing matriptase activity in healthy and maliganant colon tissue using immunofluorescence. (*Left*) H&E-stained sections. (*Center*) Matriptase visualized using the FITC channel. (*Right*) E-cadherin in the Cy3 channel. (*A*) A polyclonal antibody that recognizes a C-terminal epitope of matriptase followed by an AlexaFluor 488-labeled secondary was used to detect the total amount of matriptase in healthy human colon. *B–D* were stained with A11-AF488, specific for active matriptase. (*B*) No active matriptase was detected in healthy colon, suggesting that the matriptase in the tissue is either in zymogen form or bound to HAI-1. (*C*) Active matriptase was found in a stage II (T3N1M0) primary colon cancer section from a tissue microarray. (*D*) A hepatic metastasis section was found to contain active matriptase coexpressed with E-cadherin. The tumor tissue from this patient was used to establish the PDX model for SPECT imaging in Fig. 4. All images are shown at 40× magnification.

uptake with active matriptase levels found by quantitative mass spectrometry (Fig. 5*C*).

Discussion

This work puts forth a hypothesis suggesting that the active form of matriptase is a functional biomarker of the transformed epithelium in colon cancer and that its activity can be imaged and quantified for potential clinical benefit. Central to the detection of active matriptase, and delineation of the mechanism behind matriptase activity emerging from the epithelium, is the antibody-based probe A11. A11 is a fully human monoclonal antibody discovered previously by phage display (26). Analysis of the crystal structure of A11 bound to matriptase showed that the binding face of the antibody did not contain lysine residues (26). This allows for the modification of lysine residues for imaging without abrogating the function of the antibody. Surface plasmon resonance studies with A11 demonstrated that it was specific for the active form of matriptase and not the zymogen or the HAI-1–bound form (27). When screened against a panel of proteases, including the murine ortholog of matriptase, epithin, and other members of the TTSP family, A11 displayed no cross-reactivity (22). Taken together, we can say with certainty that in all of the experiments an active protease was specifically targeted with an accuracy not seen with other activity-based probes.

Unique to the findings of this study is that the matriptase protein level itself is not a biomarker. Matriptase is found in many normal tissues, but in an inactive form. The status of matriptase as a cancer marker is determined by its level of activity, which is directly proportional to the presence of its endogenous inhibitor, HAI-1, on the cell surface. The role that HAI-1 protein levels play in determining the presence of active matriptase on the cell surface has been analyzed in this study and a mechanism has been developed. What we can draw from this study is that, in healthy colon cells, HAI-1 and matriptase protein levels are in a delicate state of balance with no active matriptase observed on the surface of the cell. As the cells become malignant, this tenuous balance is broken; HAI-1 protein expression decreases and populations of active matriptase emerge on the cell surface. This molecular switch—that is, the decrease of HAI-1 inhibition resulting in active

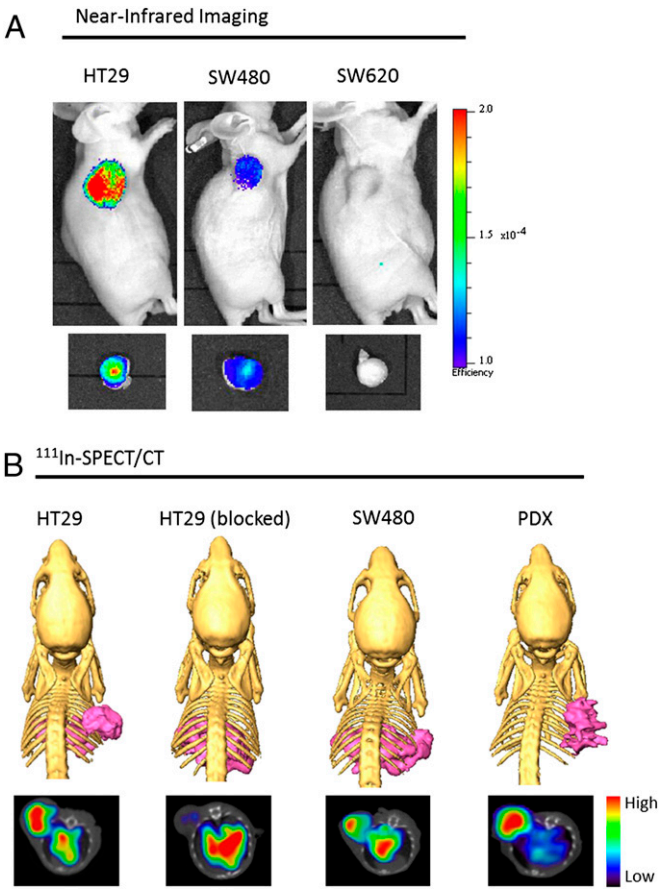

Fig. 4. Molecular imaging of active matriptase in colon cancer mouse models. (*A*) Mice bearing HT29, SW480, and SW620 xenografts were injected with 2 nmol of A11-AF680 and imaged using NIR optical imaging. The images shown are representative of $n = 3$ mice/xenograft. (*Lower*) Resected tumors showing probe tumor penetration and localization at 72 h. (*B*) SPECT imaging with ^{111}In-A11 in three xenograft models. Depicted are SPECT/CT images shown as 3D volume renderings of the SPECT data (magenta) overlaid onto surface-rendered CT data and reconstructed transverse views using a rainbow color scale to show uptake (*Lower*). (*Left to Right*) ^{111}In-A11 was administered to mice bearing HT29 xenografts, HT29 xenografts preinjected with the macromolecular matriptase inhibitor Ecotin-RR, SW480 xenografts, and a PDX model derived from resected human tumor tissue. The probe shows uptake in the HT29 xenograft, with secondary signals coming from the liver and lungs. Uptake of the probe can be blocked in the HT29 xenograft by the preinjection of ecotin engineered to be selective for matriptase. The probe accumulates preferentially in the matriptase low SW480 xenograft and in the PDX tumor. All of the images were acquired 72 h post injection and are representative of $n = 3$ mice/xenograft imaged.

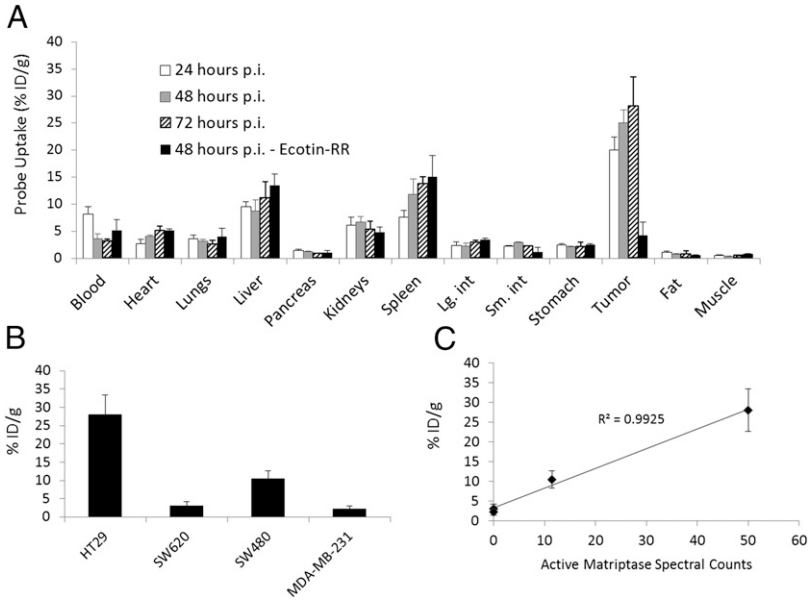

Fig. 5. Biodistribution of ^{111}In-A11 in preclinical models. (*A*) Probe distribution was determined by radioactivity assays in HT29 tumor-bearing mice ($n = 4$ for each time point). Tissues were harvested at 24, 48, and 72 h after injection of ^{111}In-A11 (25 μCi). One cohort of mice was administered matriptase-selective Ecotin-RR before injection of the probe as part of a blocking study. Shown is the Ecotin-RR blocked time point at 48h. (*B*) ^{111}In-A11 distribution at 72 h in SW620, SW480, and MDA-MB-231 xenografts ($n = 4$ mice/xenograft). (*C*) Graph demonstrating a correlation between the number of AMSCs and ^{111}In-A11 uptake in HT29 (50 AMSC), SW620 (0 AMSC), SW480 (12 AMSC), and MDA-MB-231 (0 AMSC) xenografts.

matriptase—can be detected and quantified with the active matriptase-specific antibody-based probe A11. What the A11 probe is actually measuring is not an increase in matriptase, but a decrease in HAI-1 protein. In concordance with our findings, in silico analysis of the Oncomine microarray database found that matriptase gene expression does not increase in colon cancer. During premalignant adenoma formation, however, a number of genes are methylated and epigenetically silenced, including HAI-1 (32). To date, the A11 probe is the only known example in molecular imaging where a target can be imaged with a probe only when the level of a second protein, inhibitor, or binding protein decreases.

The decrease of HAI-1 on the cell surface, resulting in active matriptase, was documented in vitro and in vivo using molecular imaging. Quantitative mass spectrometry found that, of the cancer cell lines investigated, only three had more matriptase protein than HAI-1 protein, validating the results of the live-cell imaging study with A11-AF488. Depleted cell-surface HAI-1 was qualitatively documented in vivo in HT29, SW480, and SW620 xenografts by NIR imaging. Although HT29 and SW480 had matriptase/HAI-1 protein ratios of around 1.2, they differed greatly in the number of MS2 spectral counts for active matriptase. The AMSC for HT29 was four times higher than the value for SW480: 50 versus 12. This difference correlated to a much stronger tumor uptake signal in HT29 compared with SW480. This difference was also evident in the reconstructed data showing a more intense signal in the HT29 tumor in the SPECT imaging. The active matriptase levels found by mass spectrometry in the cell lines correlated with a quantitative difference in the tumor uptake of the HT29 and SW480 xenografts (28.3% versus 12.4%). SW480 has significantly less-active matriptase, making the ^{111}In-A11 probe sensitive for cell lines with low-active matriptase. The tumors of mice treated with the macromolecular inhibitor of matriptase, Ecotin-RR, before injection of ^{111}In-A11 did not show appreciable uptake in the studies. The blocking of ^{111}In-A11 uptake by Ecotin-RR verified that probe accumulation was not due to the enhanced permeability and retention effect or other hemodynamic forces, but to the specific inhibition of active matriptase.

This study found that active matriptase on the cell surface is of clinical significance and indicative that cancer is present. Analysis of mRNA expression in healthy and diseased colon tissue found that a matriptase/HAI-1 mRNA ratio >1 is clinically significant. These data mirrored an earlier study that found the dysregulation of the matriptase/HAI-1 mRNA ratio occurred early in colon cancer tumorigenesis and was higher in adenomas and carcinomas (33). qPCR does not distinguish between zymogen and active matriptase, but immunofluorescence with A11-AF488 in tissue microarays confirmed that active matriptase was present in malignant colon cancer tissue, but absent in normal tissue where HAI-1 mRNA levels are elevated. SPECT imaging and immunofluorescence with the PDX model further confirmed active matriptase as a feature of colon cancer. Although the PDX mice imaged with SPECT were from the same patient, immunofluorescence of PDX sections from multiple patients confirmed the broad presence of active matriptase. Despite its presence on the surface of clonally derived cancer cells and tissue, the role that active matriptase plays in colon cancer and the benefit of targeting it for therapy are unknown.

The development of an imaging agent for active matriptase demonstrated an important proof of concept that a protease from a highly homologous family can be selectively targeted. Because other TTSPs are thought to be cancer biomarkers and/or to play potential roles in tumorigenesis and metastasis, a platform technology exists to selectively target them (34). Antibodies specific for active proteases on the cell surface could act as biomarker-based imaging probes for acquiring tumor information that cannot be obtained using conventional metabolic tracers. Biomarker-based imaging probes are needed to improve the risk stratification for cancer recurrence in patients following surgery or neoadjuvant therapy. In colon cancer following node-negative stage II surgery, approximately a quarter of the patients will have recurring cancer (35). Because a close association between active matriptase and stage II colon cancer has been identified, the A11 probe could be used as a noninvasive tool to detect cancer recurrence, complementing predictive RT-PCR–based assays such as OncotypeDX and ColoPrint (36). By tracking the levels of protease activity on

the cell surface of tumors with noninvasive probes, therapeutic response could be evaluated in "real time," obviating the need for secondary detection methods such as the ^{99m}Tc bone scan or ^{18}F-FDG-PET. With the ongoing development of smaller, more sensitive hand-held detectors for radionuclides and fluorophores, such probes could be used in an intraoperative setting to define tumor margins. Additionally, active-site specific probes are important tools that can unravel the role that proteases may play in the pathobiology of cancer, leading to the validation of proteases as therapeutic and/or imaging targets.

Methods

See *SI Methods* for additional methods.

Live-Cell Fluorescence Microscopy. The human cancer cell lines were plated in 35-mm glass-bottom culture dishes (MatTeK) and allowed to grow in DMEM supplemented with 1% (vol/vol) Glutamax, 10% FBS, and 1% penicillin–streptomycin until the cells were 75–90% confluent. Before imaging, the cells were washed with PBS and allowed to grow in serum-free DMEM for 18 h at 37 °C under 5% CO_2. A11-AF488 was prepared using a previously reported protocol (27). Serum-free media were removed, and the cells were washed twice with PBS before A11-AF488 in serum-free media was added to a final dye concentration of 100 nmol/L (approximate final volume was 2.3 mL). The culture dishes were returned to the incubator for 2 h, after which the plates were washed with PBS to remove any unbound antibody and 2 mL of phenol red free serum free media was added for imaging. The cells were imaged within 10 min of removal from the incubator using a Nikon 6D High Throughput Epifluorescence Microscope at the Nikon Imaging Center at the University of California at San Francisco/QB3.

In Vivo Imaging. ***NIR optical imaging.*** Mice for the optical studies were fed an alfalfa-free diet of Harlan Tekland Global 2018 to minimize background fluorescence. The mice were anesthetized with 2% isoflurane. Two nanomoles of A11-AF680, prepared as described previously, were diluted in PBS buffer and injected via the tail vein of the mice in a volume of 150–200 μL (27). Three animals from each cell-line xenograft were injected and imaged with optical imaging. Images were collected in fluorescence mode on an IVIS 50 using Living Image 2.50.2 software. Using the software, region of interest measurements were made, the fluorescence emission images were normalized to reference images, and the unitless efficiency was computed.

SPECT imaging. The chelate group for ^{111}In, DOTA–*N*-hydroxysuccinimide ester (NHS) (Macrocyclics), was attached to lysine residues on the IgG using a 25:1 molar excess of chelate in a 0.1 M $NaHCO_3$ (pH 9.0) buffer with an antibody concentration of 6 mg/mL. After 2 h of labeling at room temperature, the A11-DOTA conjugate was FPLC-purified to remove unreacted DOTA-NHS. For ^{111}In radiolabeling, $^{111}InCl_3$ was purchased from Perkin-Elmer. To radiolabel the IgG, 50 μg of A11-DOTA in 0.2 M ammonium acetate (pH 6.0) was incubated with 12 μL of $InCl_3$ (2.10 mCi) in 0.1 N HCl for 60 min at 40 °C. The product, ^{111}In-A11, was purified using a PD-10 column pre-equilibrated with PBS buffer. Labeling efficiency and purity of the product were determined using TLC. For mouse imaging, 10 μg of ^{111}In-A11, corresponding to 250–475 μCi of activity, was injected into the tail vein. The mice were imaged at 24-h intervals out to 120 h using a Gamma Medica Ideas XSPECT SPECT/CT imaging system. To block ^{111}In-A11 uptake in vivo, the macromolecular matriptase inhibitor ecotin was administered as a 200 μg i.p. bolus injection 24 h before dosing with the imaging agent. Ecotin-RR engineered for matriptase was prepared as described in a previous report (25).

ACKNOWLEDGMENTS. The authors thank Emily Bergsland, Daniel R. Hostetter, and Paco Rodriguez for helpful discussions, Mary Haak-Frendscho and Greg Landes of Takeda California for reagents and support, Kurt Thorn and Alice Thwin of the Nikon Imaging Center @ UCSF for assistance, and the Preclinical Therapeutics Core at UCSF for animal help. This work was supported by the Rogers Family Bridging the Gap Award, National Institutes of Health Grant CA128765 (to C.S.C.), and the Department of Defense Postdoctoral Prostate Cancer Award PC094386 (to A.M.L.).

1. Ii M, Yamamoto H, Adachi Y, Maruyama Y, Shinomura Y (2006) Role of matrix metalloproteinase-7 (matrilysin) in human cancer invasion, apoptosis, growth, and angiogenesis. *Exp Biol Med (Maywood)* 231(1):20–27.
2. Andreasen PA, Egelund R, Petersen HH (2000) The plasminogen activation system in tumor growth, invasion, and metastasis. *Cell Mol Life Sci* 57(1):25–40.
3. Mignatti P, Rifkin DB (1993) Biology and biochemistry of proteinases in tumor invasion. *Physiol Rev* 73(1):161–195.
4. Egeblad M, Werb Z (2002) New functions for the matrix metalloproteinases in cancer progression. *Nat Rev Cancer* 2(3):161–174.
5. Jin JS, et al. (2006) Expression of serine protease matriptase in renal cell carcinoma: Correlation of tissue microarray immunohistochemical expression analysis results with clinicopathological parameters. *Int J Surg Pathol* 14(1):65–72.
6. Uhland K (2006) Matriptase and its putative role in cancer. *Cell Mol Life Sci* 63(24): 2968–2978.
7. Tsai WC, et al. (2008) Matriptase and survivin expression associated with tumor progression and malignant potential in breast cancer of Chinese women: Tissue microarray analysis of immunostaining scores with clinicopathological parameters. *Dis Markers* 24(2):89–99.
8. Darragh MR, Bhatt AS, Craik CS (2008) MT-SP1 proteolysis and regulation of cell-microenvironment interactions. *Front Biosci* 13:528–539.
9. Tripathi M, et al. (2011) Laminin-332 cleavage by matriptase alters motility parameters of prostate cancer cells. *Prostate* 71(2):184–196.
10. Szabo R, et al. (2011) c-Met-induced epithelial carcinogenesis is initiated by the serine protease matriptase. *Oncogene* 30(17):2003–2016.
11. Oberst MD, et al. (2003) Characterization of matriptase expression in normal human tissues. *J Histochem Cytochem* 51(8):1017–1025.
12. Buzza MS, et al. (2010) Membrane-anchored serine protease matriptase regulates epithelial barrier formation and permeability in the intestine. *Proc Natl Acad Sci USA* 107(9):4200–4205.
13. Camerer E, et al. (2010) Local protease signaling contributes to neural tube closure in the mouse embryo. *Dev Cell* 18(1):25–38.
14. Parr C, Sanders AJ, Jiang WG (2010) Hepatocyte growth factor activation inhibitors: Therapeutic potential in cancer. *Anticancer Agents Med Chem* 10(1):47–57.
15. Saleem M, et al. (2006) A novel biomarker for staging human prostate adenocarcinoma: Overexpression of matriptase with concomitant loss of its inhibitor, hepatocyte growth factor activator inhibitor-1. *Cancer Epidemiol Biomarkers Prev* 15(2): 217–227.
16. Blum G, von Degenfeld G, Merchant MJ, Blau HM, Bogyo M (2007) Noninvasive optical imaging of cysteine protease activity using fluorescently quenched activity-based probes. *Nat Chem Biol* 3(10):668–677.
17. Mease RC, et al. (2008) N-[N-[(S)-1,3-Dicarboxypropyl]carbamoyl]-4-[18F]fluorobenzyl-L-cysteine, [18F]DCFBC: A new imaging probe for prostate cancer. *Clin Cancer Res* 14(10):3036–3043.
18. Smith-Jones PM, et al. (2004) Imaging the pharmacodynamics of HER2 degradation in response to Hsp90 inhibitors. *Nat Biotechnol* 22(6):701–706.
19. Ren G, et al. (2011) Non-invasive imaging of cysteine cathepsin activity in solid tumors using a 64Cu-labeled activity-based probe. *PLoS ONE* 6(11):e28029.
20. LeBeau AM, Singh P, Isaacs JT, Denmeade SR (2008) Potent and selective peptidyl boronic acid inhibitors of the serine protease prostate-specific antigen. *Chem Biol* 15(7):665–674.
21. Brown CM, et al. (2011) Peptide length and leaving-group sterics influence potency of peptide phosphonate protease inhibitors. *Chem Biol* 18(1):48–57.
22. Schneider EL, et al. (2012) A reverse binding motif that contributes to specific protease inhibition by antibodies. *J Mol Biol* 415(4):699–715.
23. Baechler S, et al. (2010) Predicting hematologic toxicity in patients undergoing radioimmunotherapy with 90Y-ibritumomab tiuxetan or 131I-tositumomab. *J Nucl Med* 51(12):1878–1884.
24. Mease RC (2010) Radionuclide based imaging of prostate cancer. *Curr Top Med Chem* 10(16):1600–1616.
25. Sun J, Pons J, Craik CS (2003) Potent and selective inhibition of membrane-type serine protease 1 by human single-chain antibodies. *Biochemistry* 42(4):892–900.
26. Farady CJ, Egea PF, Schneider EL, Darragh MR, Craik CS (2008) Structure of an Fab-protease complex reveals a highly specific non-canonical mechanism of inhibition. *J Mol Biol* 380(2):351–360.
27. Darragh MR, et al. (2010) Tumor detection by imaging proteolytic activity. *Cancer Res* 70(4):1505–1512.
28. Liu H, Sadygov RG, Yates JR III (2004) A model for random sampling and estimation of relative protein abundance in shotgun proteomics. *Anal Chem* 76(14):4193–4201.
29. Taguchi A, et al. (2011) Lung cancer signatures in plasma based on proteome profiling of mouse tumor models. *Cancer Cell* 20(3):289–299.
30. Pitteri SJ, et al. (2009) Integrated proteomic analysis of human cancer cells and plasma from tumor bearing mice for ovarian cancer biomarker discovery. *PLoS ONE* 4(11): e7916.
31. Dangles-Marie V, et al. (2007) Establishment of human colon cancer cell lines from fresh tumors versus xenografts: Comparison of success rate and cell line features. *Cancer Res* 67(1):398–407.
32. Davies RJ, Miller R, Coleman N (2005) Colorectal cancer screening: Prospects for molecular stool analysis. *Nat Rev Cancer* 5(3):199–209.
33. Vogel LK, et al. (2006) The ratio of Matriptase/HAI-1 mRNA is higher in colorectal cancer adenomas and carcinomas than corresponding tissue from control individuals. *BMC Cancer* 6:176.
34. Webb SL, Sanders AJ, Mason MD, Jiang WG (2011) Type II transmembrane serine protease (TTSP) deregulation in cancer. *Front Biosci* 16:539–552.
35. Salazar R, et al. (2011) Gene expression signature to improve prognosis prediction of stage II and III colorectal cancer. *J Clin Oncol* 29(1):17–24.
36. Kelley RK, Wang G, Venook AP (2011) Biomarker use in colorectal cancer therapy. *J Natl Compr Canc Netw* 9(11):1293–1302.